

Generation of cylindrically symmetric modes and orbital-angular-momentum modes with tilted optical gratings inscribed in high-numerical-aperture fiber

Liang Fang, Hongzhi Jia*, Hai Zhou, and Baiying Liu

Engineering Research Center of Optical Instrument and System, Ministry of Education, Shanghai Key Lab of Modern Optical System School of Optical-electrical and Computer Engineering, University of Shanghai for Science and Technology, No. 516 JunGong Road, Shanghai 200093,

China

*Corresponding author: hzjia@usst.edu.cn

Received Month X, XXXX; revised Month X, XXXX; accepted Month X, XXXX;
posted Month X, XXXX (Doc. ID XXXXX); published Month X, XXXX

Optical fiber with high numerical aperture (NA) can efficiently relieve the degeneracy of higher-order linearly polarized (LP) modes. The degeneracy relief is investigated in two types of high NA fibers, i.e., low-index cladding fiber and high-index-core fiber. A naked-core fiber, as with low-index cladding, can be used theoretically to generate the orbital-angular-momentum mode (OAMM) HE_{21} and the cylindrically symmetric modes (CSMs) TM_{01} and TE_{01} . A high-index-core fiber incorporated with high-contrast-index structure can be used similarly to obtain OAMM HE_{31} . Both the generation of CSMs and OAMMs required tilted optical gratings to couple the fundamental core mode HE_{11} into these modes. Tilt angle and modulation period of the grating fringes can be calculated simply and visually with the method proposed in this article. © 2014 Optical Society of America

OCIS codes: (060.2310) Fiber optics; (060.3735) Fiber Bragg gratings; (230.5440) Polarization-selective devices; (060.4080) Modulation

1. INTRODUCTION

Optical modes with orbital angular momentum (OAM) characterized by the term $\exp(il\phi)$ where l is the topological charge number have attracted much attention, with applications including optical communications and manipulation [1-4]. Orbital-angular-momentum modes (OAMMs) multiplexing for data transmission in fiber has developed into a promising technology with the potential to massively increase the capacity of data transmission [5, 6]. As a special case, when $l=0$ in above expression, cylindrically symmetric modes (CSMs) possess unique characteristics of polarization, including radially polarized TM_{01} modes and azimuthally polarized TE_{01} modes, and thus have been widely applied to electron acceleration [7], optical trapping [8], laser machining [9], tight focusing [10], three-Dimensional focus engineering, etc. [11, 12]. In a typical fiber, the OAMMs as vector modes are degenerated into linearly polarized (LP) modes, due to slight difference in effective refractive indices of at least two vector modes [13, 14]. Therefore, if these OAMMs can be produced in conventional fiber, it is beneficial to separate vector modes from the degenerated LP modes by enlarging the effective index differences between relevant vector modes. In precious reports, high-contrast-index ring-core-structure fiber was used to relieve mode degeneracy and generate

OAMMs and CSMs [15-17]. In this article, we investigate another method of relieving mode degeneracy with high numerical-aperture (NA) optical fiber, and thus generating CSMs and OAMMs through tilted optical gratings.

A high-NA fiber with a large normalized waveguide frequency V supports several higher-order core modes as vector modes, instead of linearly polarized (LP) modes. The conventional scalar mode LP_{11} is split into OAMM HE_{21} and either the CSMs TM_{01} or TE_{01} , LP_{21} is split into OAMMs HE_{31} and EH_{11} , in other words, the differences in effective refractive indices between these relevant modes become distinct [14]. Optical fiber gratings with tilted modulation fringes can separately couple the fundamental core mode HE_{11} into desired OAMMs, as well as CSMs TM_{01} and TE_{01} . The tilted gratings formed in high-NA fiber can be implemented using the point-by-point and phase mask techniques with interferential ultraviolet exposure or femtosecond laser pulses [18, 19]. Both the period and tilt angle of grating fringes can be determined through a visualized calculation based on the phase-matching condition and the ratio between longitudinal and transverse modulation period, respectively. This calculation provides a new sight to understand the effect of grating tilt on the coupling coefficient, apart from the previous reports through the abstract equation [20, 21].

In this article, naked-core fiber, (i.e., air-core two layered cylindrical waveguides with NA over 1 and normalized waveguide frequency V exceeding 18), is theoretically used to demonstrate a conversion from the fundamental core mode to the OAMM HE₂₁ and CSMs by using tilted optical gratings. In addition, a similar approach shows that a high-index-core fiber with a high-contrast-index structure is capable of generating OAMM HE₃₁. Naked-core fiber can be possibly fabricated by etching the cladding of a conventional fiber; high-index-core fibers may be similarly manufactured with As-Se/Ge-As-Se glasses as core/cladding waveguide materials [22], or with core/cladding materials reported in the Ref. [23]. Disregarding the weakened mechanical strength of naked-core fiber and the manufacturing challenges of these high-NA fibers, we focus on the analysis of relieving the mode degeneracy with the two types of high-NA fibers, such as a naked-core fiber and a high-index core fiber, and then theoretically generate CSMs and OAMMs HE₂₁ and HE₃₁ with mode coupling through tilted optical gratings in this article. This kind of all-fiber generation method may result in good compatibility, high conversion efficiency and purity, and simple construction, compared to the methods of generating and multiplexing OAMMs with spatial-light modulators or other free-space components and beam splitters [24, 25, 4], which may allow for practical generation and conversion of CSMs and OAMMs.

2. ANALYSIS OF RELIEVING THE MODE DEGENERACY

The division of mode degeneracy and modal dispersion are discussed in this section. The two types of high-NA fiber mentioned earlier are used for our theoretical analysis (naked-core fiber where the cladding around the general fiber is stripped, and high-contrast-index structure known as high-index-core fiber). Dispersion equations of the core modes of two-layer waveguides in fiber are listed as follows [13]:

for hybrid mode HE_{vm}/EH_{vm},

$$\left[\frac{J'_v(u_1 a_1)}{u_1 J_v(u_1 a_1)} + \frac{K'_v(w_2 a_1)}{w_2 K_v(w_2 a_1)} \right] \left[\frac{J'_v(u_1 a_1)}{u_1 J_v(u_1 a_1)} + \frac{n_2^2 K'_v(w_2 a_1)}{n_1^2 w_2 K_v(w_2 a_1)} \right] = - \left(\frac{jv\beta}{k_0 n_1 a_1} \right)^2 \left(\frac{1}{u_1^2} + \frac{1}{w_2^2} \right)^2, \quad (1)$$

for mode TE₀₁,

$$\frac{K'_0(w_2 a_1)}{w_2 K_0(w_2 a_1)} + \frac{J'_0(u_1 a_1)}{u_1 J_0(u_1 a_1)} = 0, \quad (2)$$

and for mode TM₀₁,

$$\frac{K'_0(w_2 a_1)}{w_2 K_0(w_2 a_1)} + \frac{n_1^2 J'_0(u_1 a_1)}{n_2^2 u_1 J_0(u_1 a_1)} = 0, \quad (3)$$

where $u_1 = k_0 \sqrt{n_1^2 - n_{eff}^2}$ and $w_2 = k_0 \sqrt{n_{eff}^2 - n_2^2}$, $k_0 = 2\pi/\lambda$ and $\beta = k_0 n_{eff}$ present the wave vector and the propagation constant of light, respectively; n_1, n_2 and n_{eff} are the refractive indices of the inner and outer layer waveguides, and the effective indices of guided mode, respectively; a_1 is

the core radius, and the integers v and m denote the mode ordinal and corresponding radial ordinal.

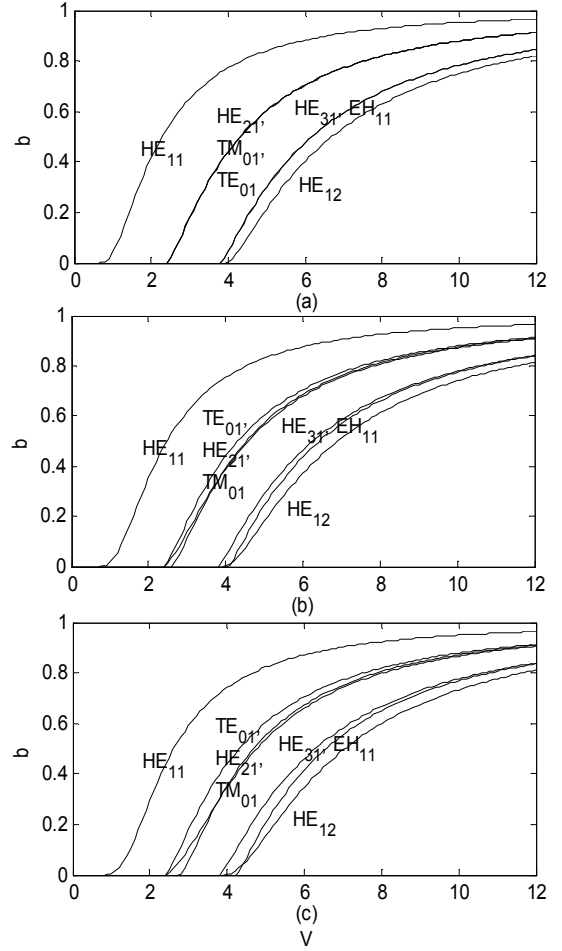


Fig. 1 Modal dispersion curves of several vector modes, (a) ordinary SMF, $n_1=1.4681$, $n_2=1.4628$; (b) high-index-core fiber $n_1=1.85$, $n_2=1.46$; (c) naked-core fiber, $n_1=1.4681$, $n_2=1.00$.

The fiber parameters of the high NA-fibers are $n_1=1.4681$ and $n_2=1.00$ for a naked-core fiber, $n_1=1.85$ and $n_2=1.46$ for a high-index-core fiber, both with a core radius $a_1=4.15 \mu\text{m}$. The dispersion curves of several vector modes including HE₁₁, HE₂₁, TM₀₁, TE₀₁, HE₃₁, EH₁₁, and HE₁₂ are depicted in Fig. 1(a) for an ordinary single-mode fiber (SMF), those of a high-index-core fiber are depicted in Fig. 1(b), and those of a naked-core fiber are depicted in Fig. 1(c). In the figure, the variable $b = (n_{eff}^2 - n_2^2)/(n_1^2 - n_2^2)$ indicates the normalized effective refractive index, $V = k_0 a_1 \sqrt{n_1^2 - n_2^2}$ is the normalized waveguide frequency that becomes a function depending solely on the operating wavelength λ and the core radius a_1 . Note that the dispersion curves of other higher-order vector modes, if supported, are not included in Fig. 1. In general, it can be seen that the dispersion curves of OAMMs HE₂₁, HE₃₁ and EH₁₁, CSMs TM₀₁ and TE₀₁ are almost completely split in high NA fibers shown in Fig. 1(b) and 1(c), compared with those in Fig. 1(a). This situation can be explained by the large ratio between n_1^2 and n_2^2 in Eqs. (1) and (3); in other words, the splitting is caused by a high NA = $\sqrt{n_1^2 - n_2^2}$, which reaches 1.14 for a high-index-

core fiber and 1.07 for a naked-core fiber, but only 0.12 for the SMF.

In order to reveal the effective index differences between the fundamental core mode HE₁₁ and each vector mode under various NA for both high-index-core fiber and low-index-cladding fiber, which directly determines the dispersion degree for mode coupling from HE₁₁ to other modes, according to Eqs. (1), (2) and (3), we define a function of the effective index n_{eff} relative to NA ,

$$n_{eff}^i = f_i(NA), \quad (4)$$

with $i=11$, for HE₁₁; $i=21$, for HE₂₁; $i=m01$, for TM₀₁; for TE₀₁, $i=e01$, for HE₃₁, $i=31$; for EH₁₁, $i=h11$; for HE₁₂, $i=12$. Then the Δn_{eff} of mode couples stemming from HE₁₁, combined with HE₂₁, TM₀₁, TE₀₁, HE₃₁, EH₁₁, and HE₁₂, can be expressed as follows:

$$\Delta n_{eff}^{11-i} = f_{11} - f_i. \quad (i \neq 11) \quad (5)$$

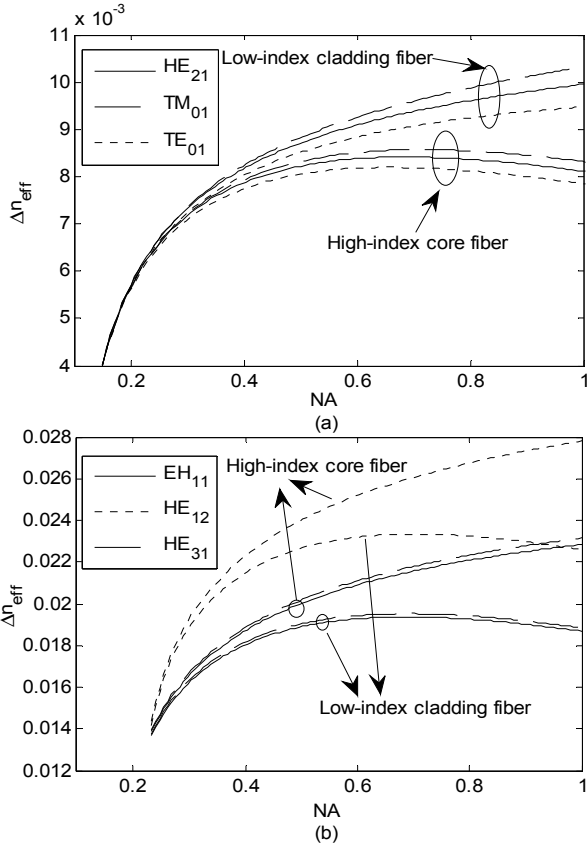


Fig. 2 Relationships between different Δn_{eff} under various NA for HE₂₁, TM₀₁, TE₀₁ (a), and HE₃₁, EH₁₁, and HE₁₂ (b) in both high-index core and low-index cladding fiber.

In Fig. 2(a), three kinds of Δn_{eff}^{11-i} for HE₂₁, TM₀₁, TE₀₁ are illustrated for high-index-core fiber with a fixed index $n_2=1.46$; and for low-index-cladding fiber with a fixed index $n_1=1.46$, both under the parameters of $a_1=4150$ nm and $\lambda=1550$ nm. It can be seen that the three Δn_{eff} are obviously separated with increasing NA , and the degree of separation in the low-index-cladding fiber is more distinct than in the high-index-core fiber. Similarly, the other three kinds of Δn_{eff}^{11-i} for HE₃₁, EH₁₁, and HE₁₂

are shown in Fig. 2(b). We can see that the effect of NA on separation of Δn_{eff}^{11-31} and Δn_{eff}^{11-h11} is slight when NA increases beyond a certain point.

3. MODE COUPLING WITH TILTED OPTICAL GRATINGS

In this section, naked-core fiber and high-index-core fiber are used to achieve mode conversion from the fundamental core mode HE₂₁ to CSMs TM₀₁, and TE₀₁, and OAMMs HE₂₁ and HE₃₁ using tilted optical gratings. Based on the coupled-mode theory [26], coupling via an optical fiber grating must satisfy two requirements, the phase-matching condition must be met, and a large coupling coefficient between the two related modes is required. For the phase-matching condition of transmissive optical gratings,

$$\frac{2\pi}{\lambda} \Delta n_{eff} = \frac{2\pi}{\Lambda_0}, \quad (6)$$

where Λ_0 is the grating period, and Δn_{eff} is the difference in the two modes' effective refractive indices. For obtaining CSMs and OAMM HE₂₁ with naked-core fiber, we substitute the independent variable NA for V/NA where $NA=1.07$, while for OAMM HE₃₁ with high-index core fiber, $NA=1.14$, the function in Eq. (4) then becomes

$$n_{eff}^i = f_i(V/NA), \quad (7)$$

Inserting Eqs. (5) and (7) into Eq. (6), and multiplying the new equation by core radius r on both sides, yield a new expression involving the variable Λ, r and λ

$$\frac{2\pi r}{\Lambda_0} = \frac{2\pi r}{\lambda} \left[f_{11} \left(\frac{2\pi r}{\lambda} \right) - f_i \left(\frac{2\pi r}{\lambda} \right) \right]. \quad (i \neq 11) \quad (8)$$

The relevant expression in Eq. (8) plays a significant role on determining the grating period in the case of different core radius and operating wavelength.

The coupling coefficient is expressed by [27]

$$\kappa_{11-i} = \frac{1}{2} \omega \epsilon_0 n_1^2 \bar{\delta} \int_0^{2\pi} d\phi \int_0^{a_1} \exp(Kr \cos \phi \tan \theta) E_{11} E_i^* r dr, \quad (9)$$

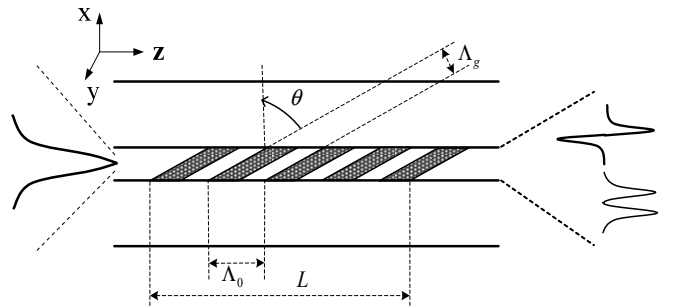


Fig. 3 Structure diagram of tilted optical gratings in a high-NA fiber, and the coupling process from the fundamental mode HE₁₁ (left) to vector modes TM₀₁, TE₀₁, HE₂₁ or HE₃₁ (right).

where ω and ϵ_0 are the angular frequency and the dielectric constant in vacuum, $\bar{\delta}$ is the average modulation strength, E_{11} and E_i are functions of electric field

transverse distribution of the mode HE_{11} ; HE_{21} when $i = 21$; TM_{01} when $i = m01$; TE_{01} when $i = e01$, HE_{31} when $i = 31$; EH_{11} when $i = h11$; and HE_{12} when $i = 12$, the superscript* indicates a complex conjugate, $K = 2\pi/\Lambda_0$ is the grating constant, and θ is the tilt angle of gratings.

The structure diagram of tilted optical gratings written in high- NA fibers including a naked-core fiber and a high-index-core fiber are demonstrated in Fig. 3, where a mode conversion is observed from the fundamental mode HE_{11} to CSMs TM_{01} and TE_{01} , and OAMMs HE_{21} and HE_{31} . Note that the field distributions are described by the electric field intensities with direction indication. In Eq. (9), with tilted gratings, it is the transverse modulation period $\Lambda_x = \Lambda_0/\tan\theta$ that acts on the expression for the coupling coefficient where $r\cos\phi$ implies the displacement in the direction of transverse modulation.

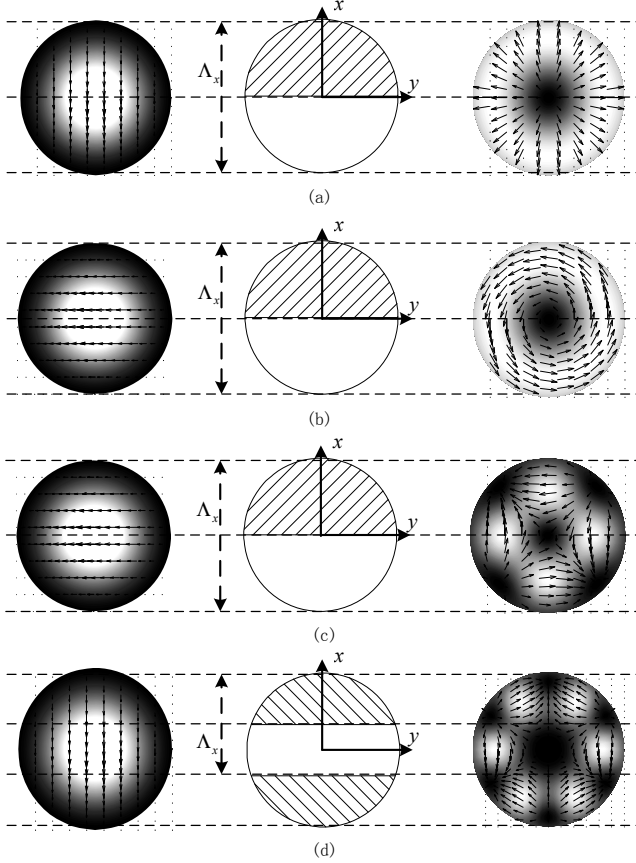


Fig. 4 Relationships between transverse modulation period Λ_x and mode coupling from HE_{11} to TM_{01} (a), to TE_{01} (b), to HE_{21} (c), and to HE_{31} (d).

To maximize the integral value when efficiently obtaining CSMs and OAMM HE_{21} with a naked-core fiber, the maximum coupling coefficient from HE_{11} to these modes occurs with a transverse modulation period $\Lambda_x \approx 2a_1$. The relationship between the field distributions of HE_{11} coupled with CSMs and OAMM HE_{21} are illustrated in Fig. 4(a)-(c), along with the transverse modulation fringes. In conventional fiber, i.e., a weakly guiding fiber, HE_{21} coupled from HE_{11} will be degenerated into LP_{11} with TM_{01} , or into its cross-polarization LP_{11} with TE_{01} , which has been previously reported [28]. In our previous work, we

have revealed the mode coupling between two core modes LP_{0m} , as well as between higher-order core modes LP_{0m} and cladding modes HE_{1m} [29, 30]. Here, for the tilted gratings, the tilt angle θ and actual grating period Λ_g can be visually calculated by

$$\theta = \tan^{-1}\left(\frac{\Lambda_0}{\Lambda_x}\right). \quad (10)$$

$$\Lambda_g = \Lambda_0 \cos\theta$$

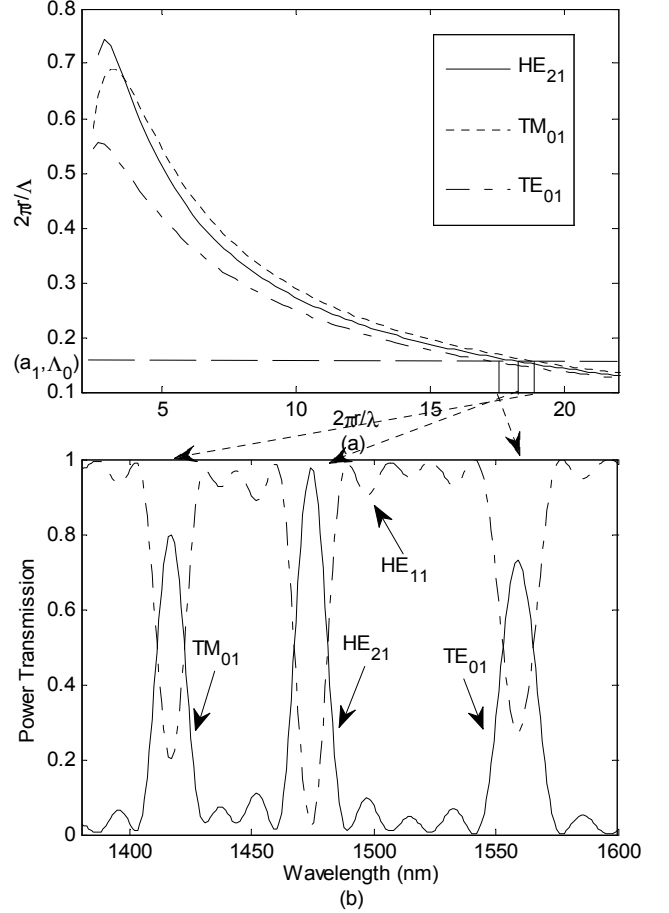


Fig. 5 (a) Curves of $2\pi r/\Lambda$ versus $2\pi r/\lambda$ for CSMs and OAMM HE_{21} coupled from HE_{11} in a naked-core fiber. (b) Power exchange spectrum from HE_{11} to these three modes.

According to Eqs. (1)-(3), (7) and (8), the curves of $2\pi r/\Lambda$ versus $2\pi r/\lambda$ expressed by Eq. (8) for CSMs and OAMM HE_{21} are depicted in Fig. 5(a). From this, the grating period Λ_0 can be determined for desired CSMs and OAMM HE_{21} at any operating wavelength. Then the actual grating period Λ_g and tilt angle can be obtained based on Eq. (10). Here if power exchanges of these three modes fall within the wavelength range of 1400-1580nm, and the core radius of fiber are taken as 4150nm, the corresponding actual grating period Λ_g and tilt angle can be calculated (see Table 1). This table also contains the normalization coupling coefficients based on Eq. (9) and the product between the optional grating length and modulation strength in the case of maximum coupling efficiency determined by $\eta = \sin^2(\kappa L/2) = 1$ [26]. Power conversion

spectrum from HE₁₁ to CSMs and OAMM HE₂₁ are depicted in Fig. 5(b). Note that the input polarization of the fundamental core mode HE₁₁ for the wavelength of 1420 nm needs to be orthogonal to the wavelength of 1560 nm, which is expounded in Fig. 4(a) and 4(b). From the Fig. 5(b), we can see that the vector modes HE₂₁, TM₀₁ and TE₀₁ are completely split in the transmission spectrum, and have high efficiency of power exchanges. Actually, the efficiency can be controlled by adjusting modulation strength or the grating length for individual CSM TM₀₁ or TE₀₁ or OAMM HE₂₁.

Tab. 1 Grating parameters of tilted optical gratings and corresponding coupling coefficients

λ (nm)	1417	1475	1560	1537
	TM ₀₁	HE ₂₁	TE ₀₁	HE ₃₁
Λ_g (um)	8.29			5.52
θ	87.08°			86.30°
k/δ (um ⁻¹)	2.09	2.69	1.95	2.17
δL (um)	1.05			1.45

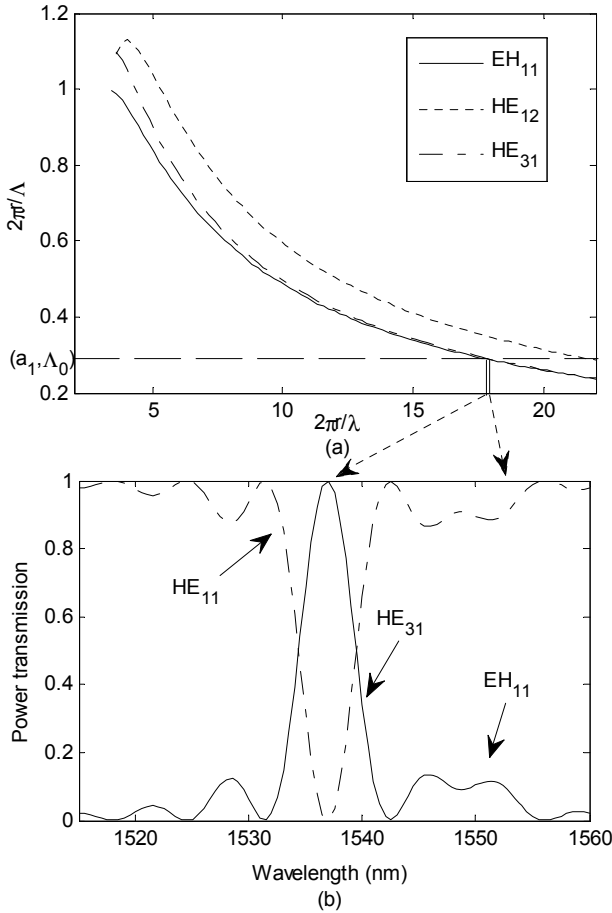


Fig. 6(a) Curves of $2\pi r/\Lambda$ versus $2\pi r/\lambda$ for OAMM HE₃₁, EH₁₁, and HE₁₂ coupled from HE₁₁ in a high-index core fiber. (b) Power exchange spectrum from HE₁₁ to OAMM HE₃₁.

Similarly, to obtain OAMM HE₃₁ for a high-index-core

fiber, while maximizing the coupling coefficient, the transverse modulation period should be $\Lambda_x \approx 4a_1/3$. Fig. 4(d) illustrates the relationship between the field distributions for HE₁₁, OAMM HE₃₁ and the transverse modulation fringes. The curves of $2\pi r/\Lambda$ versus $2\pi r/\lambda$ expressed by Eq. (8) for OAMMs HE₃₁, EH₁₁, and HE₁₂ with second radial order are depicted in Fig. 6(a). The parameters calculated similarly are listed in Table 1. Power conversion spectrum from HE₁₁ to OAMM HE₃₁ is presented in Fig. 6(b). Note that for this spectrum, mode EH₁₁ has a low conversion rate because of the small coupling coefficient owing to the transverse modulation period shown in Fig. 5(d). Moreover, the point of power conversion from HE₁₁ to HE₂₁ is beyond the wavelength range of the spectrum in Fig. 6(b). Other higher-order OAMMs can be converted from the fundamental core mode HE₁₁ by similar methods, provided the gratings' longitudinal modulation period meets the phase-matching condition. Meanwhile, the transverse modulation fringes are adjusted to make the coupling coefficients between HE₁₁ and desired OAMMs sufficiently large.

4. SUMMARY

High-NA fiber has been studied in this article as a means for generating and transmitting CSMs and OAMMs. The NA can be greatly increased by increasing or decreasing a fiber's core and cladding indices. Mode degeneracy is relieved in the high-NA fiber so that the scalar mode LP₁₁ is divided into CSMs and OAMM HE₂₁, and LP₂₁ mode is divided into OAMMs HE₃₁ and EH₁₁. These CSMs and OAMMs can be generated by tilted optical gratings inscribed in this high-NA fiber. In this article, naked-core fiber was used with such gratings to achieve theoretical generation of CSMs and OAMM HE₂₁, coupled with the fundamental core mode HE₁₁. Similarly, OAMM HE₃₁ is obtained with tilted optical gratings inscribed in high-index-core fiber, and this method may be expanded for the generation of other higher-order OAMMs.

ACKNOWLEDGEMENT

This work is supported by the National Basic Research Program of China (2013CB707500), the Innovation Fund Project for Graduate Student of Shanghai (JWCXSL1302), and partly supported by the Shanghai Leading Academic Discipline Project (No.S30502).

REFERENCES

1. K. Dholakia, G. Spalding, and M. MacDonald, "Optical tweezers: the next generation," *Physics World*, 31-35 (2002).
2. S. Franke-Arnold, L. Allen, and M. Padgett, "Advances in optical angular momentum," *Laser & Photon. Rev.* **2**, 299-313 (2008).
3. Q. Zhan, "Cylindrical vector beams: from mathematical concepts to applications," *Adv. Opt. Photonics* **1**, 1-57 (2009).
4. J. Wang, J. Yang, I. M. Fazal, N. Ahmed, Y. Yan, H. Huang, Y. Ren, Y. Yue, S. Dolinar, M. Tur, and A. E. Willner, "Terabit free-space data transmission employing orbital angular momentum multiplexing," *Nature Photon.* **6**, 488-496 (2012).

5. N. Bozinovic, Y. Yue, Y. Ren, M. Tur, P. Kristensen, A.E. Willner, S. Ramachandran, "Orbital angular momentum (OAM) based mode division multiplexing (MDM) over a Km-length Fiber," ECOC Postdeadline Papers © 2012 OSA.
6. N. Bozinovic, Y. Yue, Y. X. Ren, M. Tur, P. Kristensen, H. Huang, A. E. Willner, and S. Ramachandran, "Terabit-scale orbital angular momentum mode division multiplexing in fibers," *Science* **340**, 1545-1548 (2013).
7. Y. I. Salamin, "Electron acceleration from rest in vacuum by an axicon Gaussian laser beam," *Phys. Rev. A* **73**, 043402 (2006).
8. Q. Zhan, "Trapping metallic Rayleigh particles with radial polarization," *Opt. Express* **12**, 3377-3382 (2004).
9. M. Meier, V. Romano, and T. Feurer, "Material processing with pulsed radially and azimuthally polarized laser radiation," *Appl. Phys. A* **86**, 329-334 (2007).
10. B. Hao and J. Leger, "Experimental measurement of longitudinal component in the vicinity of focused radially polarized beam," *Opt. Express* **15**, 3550-3556 (2007).
11. W. Chen and Q. Zhan, "Three-dimensional focus shaping with cylindrical vector beams," *Opt. Commun.* **265**, 411-417 (2006).
12. M. A. Ahmed, A. Voss, M. M. Vogel, and T. Graf, "Multilayer polarizing grating mirror used for the generation of radial polarization in Yb:YAG thin-disk lasers," *Opt. Lett.* **32**, 3272-3274 (2007).
13. C. Tsao, *Optical Fibre Waveguide Analysis*, (Oxford University, 1992), Part 3.
14. K. Okamoto, *Fundamentals of Optical Waveguides*, (Elsevier Academic Press, 2006), Chap. 3.
15. Y. Yan, Y. Yue, H. Huang, J. Yang, M. R. Chitgarha, N. Ahmed, M. Tur, S. J. Dolinar, and A. E. Willner, "Efficient generation and multiplexing of optical orbital angular momentum modes in a ring fiber by using multiple coherent inputs," *Opt. Lett.* **37**, 3645-3647 (2012).
16. Y. Yue, Y. Yan, N. Ahmed, J. Yang, L. Zhang, Y. Ren, H. Huang, K. M. Birnbaum, B. I. Erkmen, S. Dolinar, M. Tur, and A. E. Willner, "Mode properties and propagation effects of optical orbital angular momentum (OAM) modes in a ring fiber," *IEEE Photon. J.* **4**, 535-543 (2012).
17. S. Ramachandran, P. Kristensen, and M. F. Yan, "Generation and propagation of radially polarized beams in optical fibers," *Opt. Lett.* **34**, 2525-2527 (2009).
18. J. Thomas, e.wikszak, T. clausnitzer, U. Fuchs, U. Zeitner, S. nolte, and A. Tunnermann, "Inscription of fiber Bragg gratings with femtosecond pulses using a phase mask scanning technique," *Appl. Phys. A* **86**, 153-157 (2007).
19. R. J. Williams, R. G. Krämer, S. Nolte, and M. J. Withford, "Femtosecond direct-writing of low-loss fiber Bragg gratings using a continuous core-scanning technique," *Opt. Lett.* **38**, 1918-1920 (2013).
20. K. S. Lee, "Mode coupling in tilted planar waveguide gratings," *Appl. Opt.* **39**, 6144-6149 (2000).
21. A. E. Lobo, C. M. Sterke, and J. A. Besley, "N-fold symmetric gratings as gain-flattening filters," *J. Lightwave Technol.* **23**, 1441-1448 (2005).
22. I. Kubat, C. S. Agger, U Møller, A. B. Seddon, Z. Tang, S. Sujecki, T. M. Benson, D. Furniss, S. Lamrini, K. Scholle, P. Fuhrberg, B. Napier, M. Farries, J. Ward, P. M. Moselund, and O. Bang, "Mid-infrared supercontinuum generation to 12.5µm in large NA chalcogenide step-index fibres pumped at 4.5µm," *Opt. Express* **22**, 19169-19182 (2014).
23. Y. Yan, L. Zhang, J. Wang, J. Yang, I. M. Fazal, N. Ahmed, A. E. Willner, and S. J. Dolinar, "Fiber structure to convert a Gaussian beam to higher order optical orbital angular momentum modes," *Opt. Lett.* **37**, 3294-3296 (2012).
24. J. Arlt, K. Dholakia, L. Allen, and M. Padgett, "The production of multiringed Laguerre-Gaussian modes by computer-generated holograms," *J. Mod. Opt.* **45**, 1231-1237 (1998).
25. G. Gibson, J. Courtial, M. J. Padgett, M. Vasnetsov, V. Pas'ko, S. M. Barnett, and S. Franke-Arnold, "Free-space information transfer using light beams carrying orbital angular momentum," *Opt. Express* **12**, 5448-5456 (2004).
26. T. Erdogan, "Fiber Grating Spectra," *J. Lightwave Technol.* **15**, 1277-1294 (1997).
27. T. Erdogan and J. E. Sipe, "Tilted fiber phase gratings," *J. Opt. Soc. Am. A* **13**, 296-313 (1996).
28. K. S. Lee and T. Erdogan, "Fiber mode conversion with tilted gratings in an optical fiber," *J. Opt. Soc. Am. A* **18**, 1176-1185 (2001).
29. L. Fang, H. Jia, "Coupling analyses of LP_{0m} modes with optical fiber gratings in multimode fiber and their application in mode-division multiplexing transmission," *Opt. Commun.* **322**, 118-122 (2014).
30. L. Fang, H. Jia, "Mode add / drop multiplexers of LP₀₂ and LP₀₃ modes with two parallel combinative long-period fiber gratings," *Opt. Express* **22**, 11488-11497 (2012).